Supporting Information

Lautenschläger et al. 10.1073/pnas.0811261106

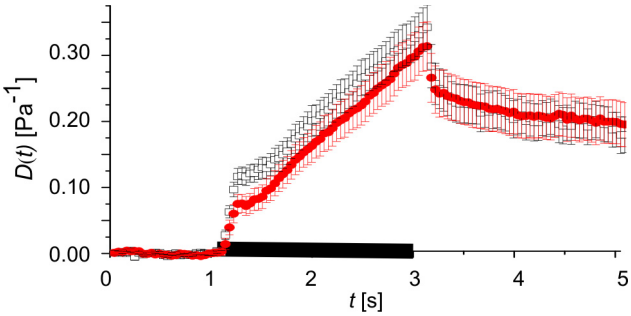

Fig. S1. Compliance measurements with the μOS. The response of a cell to a constant stress is a viscoelastic, retarded elongation expressed as the creep compliance, $D(t)$. The duration of stress application is indicated by a black bar on the time axis. Once the stress is released the cell relaxes. Displayed are APL cells from the same sample measured after 24 h. There are no significant differences between the two measurements demonstrating the reproducibility of this mechanical analysis with μOS. Symbols represent: (filled circles) APL cells (t = 0 h, n = 26), (open squares) APL cells (t = 24 h, n = 25). Data points are mean ± SEM.

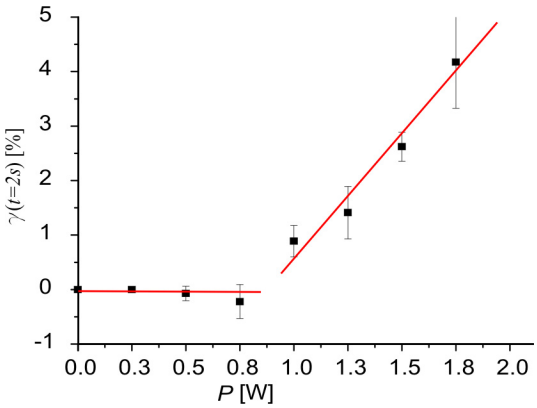

Fig. S2. Deformability measurements of APL cells at different applied laser powers. APL cells were subjected to different laser powers and therefore different stresses in the μOS to test the linearity of the response. The deformability after 2 s of stretch is given in units of relative strain $\gamma(t = 2s) = \Delta r(t = 2s)/r_0$. This analysis showed that a certain threshold power ($P \approx 0.75$ W) is needed to deform cells. Afterward the deformation is approximately linear. The power quoted is the power per beam incident on the cells from one side.

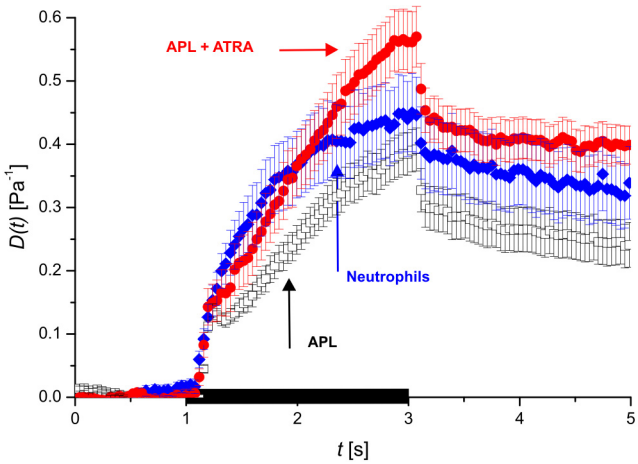

Fig. S3. Compliance of APL cells compared to neutrophils. The compliance of neutrophils (filled diamonds, $n = 17$) is higher than that of untreated APL cells (open squares, $n = 42$), but lower in comparison to ATRA differentiated APL cells (filled circles, $n = 44$). The duration of stress application is indicated by the black bar on the time axis. Data show mean ± SEM.

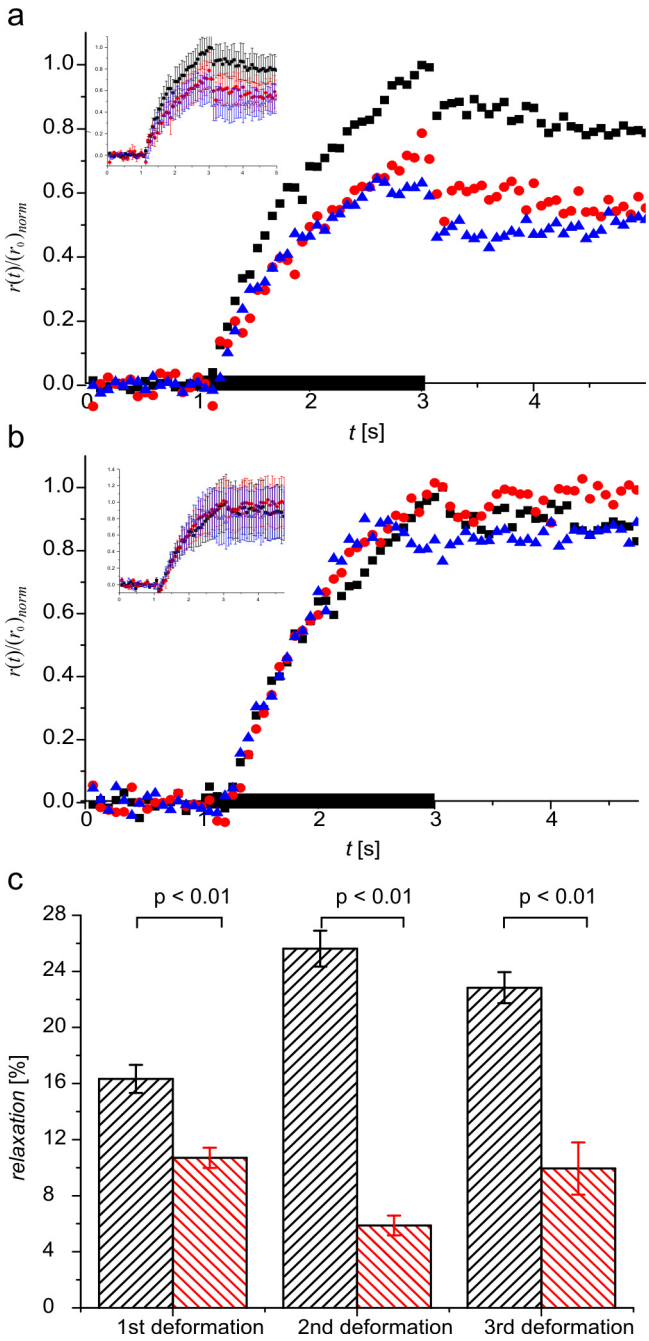

Fig. S4. Repeated deformability measurements of differentiated APL cells. The same cells were deformed three times for 2 s with 60 s in-between. Measurements were normalized to the maximum relative deformation of the first deformation of each cell type. The relaxation behavior was similar in all three stretches for differentiated APL cells (*A*). Differentiated APL cells treated with paclitaxel (*B*) showed a decreased relaxation in all three stretches. These differences in the relaxation behavior between differentiated APL cells with and without paclitaxel is significant in all three stretches (*C*). Measured cell numbers were n = 9, n = 8, and n = 14 for differentiated APL cells during the first (filled squares), second (filled circles), and third (filled triangles) stretch and n = 9, n = 7, and n = 7 for differentiated APL cells treated with paclitaxel during the first (filled squares), second (filled circles), and third (filled triangles) stretch, respectively. Insets show the same graphs with SEM.

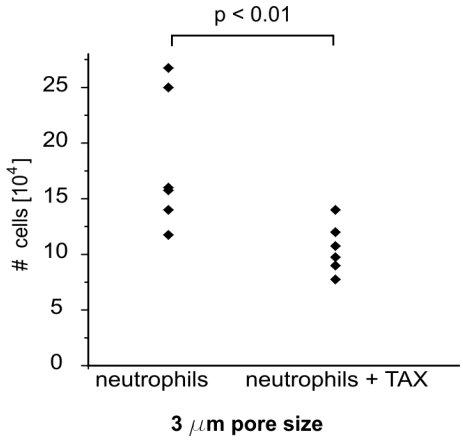

Fig. S5. Chemotaxis of human neutrophils. The number of neutrophils migrating through 3-μm pores after 3 h is significantly decreased after treatment with paclitaxel (TAX). The experiment was performed six times.

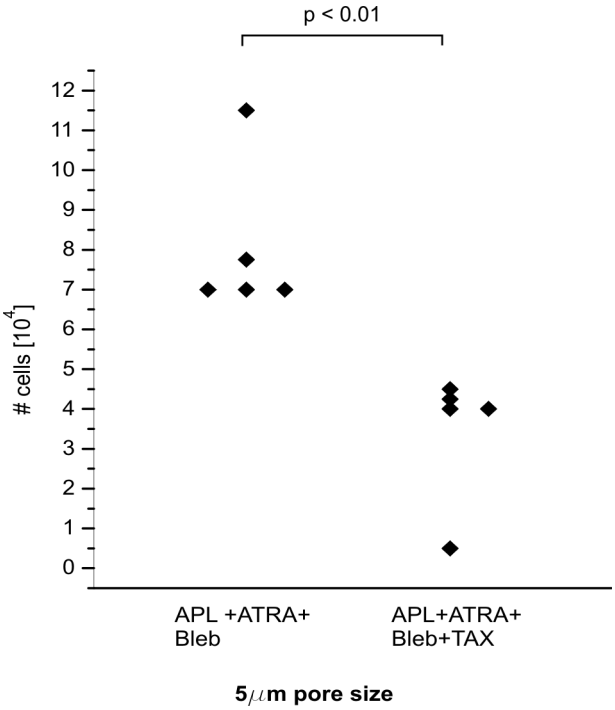

Fig. S6. Chemotaxis of differentiated APL cells through 5-μm pores after exposure to 100 μM blebbistatin (Bleb). The addition of 5 μM paclitaxel (TAX) significantly impedes migration in comparison to APL cells treated only with blebbistatin. The experiment was performed five times.

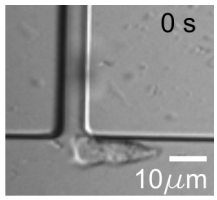

Movie S1. Migration of differentiated APL cell into microchannel. Video-microscopic recording of the chemotactic migration of an APL cell differentiated with ATRA into a PDMS channel with 7-μm width and 8-μm height.

Movie S1 (AVI)

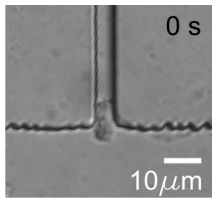

Movie S2. Migration of differentiated APL cell treated with paclitaxel into microchannel. Video-microscopic recording of the chemotactic migration of an APL cell differentiated with ATRA and treated with paclitaxel into a PDMS channel with 7-μm width and 8-μm height.

Movie S2 (AVI)